Available online at www.sciencedirect.com

ScienceDirect

Nuclear Physics A 967 (2017) 301–304

NUCLEAR PHYSICS A

www.elsevier.com/locate/nuclphysa

System-size dependence of the charged-particle pseudorapidity density at $\sqrt{s_{\rm NN}} = 5.02$ TeV with ALICE

Christian Holm Christensen

(for the ALICE Collaboration)[1]

Niels Bohr Institute, University of Copenhagen, Blegdamsvej 17, DK-2100 Copenhagen

Abstract

We present the charged-particle pseudorapidity density in pp, p–Pb, and Pb–Pb collisions at $\sqrt{s_{\rm NN}} = 5.02$ TeV over a broad pseudorapidity range. The distributions are determined using the same experimental apparatus and methodologies, thereby minimizing systematic uncertainties, and providing clear and model-independent observations on the system-size dependence of the particle production at relativistic energies. An increase of particle production in Pb–Pb collisions near mid-rapidity, relative to pp collisions, is observed. The relative linearity in p–Pb collisions of the ratio to the smaller system indicate a coherent particle production throughout the longitudinal extend of the collision zone.

1. Introduction

With the Pb–Pb and pp collisions provided by the Large Hadron Collider at a collision energy of $\sqrt{s_{\rm NN}} = 5.02$ TeV in 2015, and the p–Pb collisions provided in 2013, it is for the first time possible to compare the 3 collisions systems at the same ultrarelativistic energies. In this proceeding, we compare the primary charged-particle pseudorapidity density ($\mathrm{d}N_{\rm ch}/\mathrm{d}\eta$) of all three collision systems over a wide pseudorapidity (η) range of $-3.5 < \eta < 5$ using data from ALICE.

The primary charged-particle pseudorapidity density for different collision systems provides a first-order insight into the production of particles. By comparing the distributions from various collision systems, we can learn about the production mechanisms, in particular how the nuclear medium affects these mechanisms. A primary, charged particle is a charged particle with a mean proper lifetime τ larger than 1 cm/c, which is either a) produced directly in the interaction, or b) from decays of particles with τ smaller than 1 cm/c. In this proceeding all quantities reported are for primary, charged particles, although we will omit "primary" for brevity.

A detailed description of ALICE and its performance can be found elsewhere [1]. Brief descriptions of the four detectors used for this analysis: SPD, FMD, V0, and ZDC, are available in a recent publication by ALICE [2].

[1] *Email address:* cholm@nbi.dk

http://dx.doi.org/10.1016/j.nuclphysa.2017.05.066

2. Data sample, analysis method, and systematic uncertainties

The results presented here are based on data collected by ALICE in 2013 during the p–Pb collisions, and in 2015 during the pp and Pb–Pb collision run of the LHC, both at $\sqrt{s_{\rm NN}} = 5.02\,\text{TeV}$. About 100 000 events with a minimum bias trigger requirement [3] were analysed in the centrality range from 0% to 90% and 0% to 100% for Pb–Pb and p–Pb, respectively. The minimum bias trigger for p–Pb and Pb–Pb collisions in ALICE is defined as a coincidence between the A ($z > 0$) and C ($z < 0$) sides of the V0 detector. Likewise, for the pp collisions about 100 000 events with a minimum bias trigger requirement *and* at least one charged particle in $|\eta| < 1$ were analyzed [4]. The minimum bias condition for pp collisions in ALICE is defined as the three-fold inclusive logical *or* between the A and C sides of the V0 detector, and the fast trigger signal from the SPD ($|\eta| \lesssim 1.5$). By requiring at least one charged particle at mid-rapidity, the so-called INEL>0 event class, we reduce the systematic uncertainty related to absolute normalization to the full inelastic cross-section, while still sampling a large fraction of the hadronic cross-section.

The standard ALICE event selection [5] and centrality estimator based on the V0–amplitude [6, 7] are used in this analysis. The event selection consists of: exclusion of background events using the timing information from the ZDC (for Pb–Pb and p–Pb) and V0 detectors; verification of the trigger conditions; and a reconstructed position of the collision. In Pb–Pb collisions, the $(90-100)\%$ centrality class has substantial contributions from electromagnetic processes and is therefore not included in the results presented here [6].

The analysis method used is identical to what has previously been presented [2]. The measurement of the charged-particle pseudorapidity density at mid-rapidity ($|\eta| < 2$) is obtained from a tracklet analysis using the two layers of the SPD. In the forward regions ($-3.5 < \eta < -1.8$ and $1.8 < \eta < 5$), the measurement is provided by the analysis of the deposited energy signal in the FMD: a statistical approach to calculate the inclusive number of charged particles; and a data-driven correction — derived from previous satellite–main collisions — to remove the large background from secondary particles.

Sources and dependencies of the systematic uncertainties for the measurements at mid-rapidity are detailed elsewhere [2, 4, 7]. For pp, the systematic uncertainties amount to 1.5% over all η; for p–Pb: 2.7%, likewise over all η, while for Pb–Pb the total systematic uncertainties are 2.6% at $\eta = 0$ and 2.9% at $|\eta| = 2$. The systematic uncertainty is mostly correlated over $|\eta| < 2$, and largely independent of centrality. The evaluation of systematic uncertainties in the forward direction employs the same technique as for previous results [2]. The uncertainty is the same for all collision systems and is uncorrelated across η, amounting to 6.9% for $\eta > 3.5$ and 6.4% elsewhere within the forward regions.

The systematic uncertainty on $\mathrm{d}N_{\rm ch}/\mathrm{d}\eta$ due to the centrality class definition in Pb–Pb is estimated to be 0.6% for the most central and 9.5% for the most peripheral class [8]. The $(80-90)\%$ centrality class has residual contamination from electromagnetic processes detailed elsewhere [6], which gives rise to a 4% additional systematic uncertainty in the measurements. For p–Pb collisions, the systematic uncertainty due to the centrality classification amounts to 1.5% and 2% in centrality ranges $(0-40)\%$ and $(40-100)\%$, respectively [7].

3. Results

The left column of Fig. 1 shows the charged-particle pseudorapidity density in pp, p–Pb, and Pb–Pb [2] collisions at $\sqrt{s_{\rm NN}} = 5.02\,\text{TeV}$. For Pb–Pb we see an increase of two orders of magnitude from the most peripheral to the most central events, while for p–Pb the increase is more moderate. For p–Pb collisions, the lead ion travels toward positive η, the proton towards negative η, and the rapidity of the center-of-mass system in the laboratory frame is $y_{\rm CM} = 0.465$. The middle and bottom rows of the right column of Fig. 1 shows the ratio of the charged-particle pseudorapidity density in p–Pb and Pb–Pb collisions to the charged-particle pseudorapidity density in pp collisions, all at the same collision energy of $\sqrt{s_{\rm NN}} = 5.02\,\text{TeV}$,

$$r_X = \frac{\mathrm{d}N_{\rm ch}/\mathrm{d}\eta|_X}{\mathrm{d}N_{\rm ch}/\mathrm{d}\eta|_{\rm pp}}$$

were X labels centrality classes in p–Pb and Pb–Pb. In these ratios, systematic uncertainties are partially canceled, and the magnitude of the resulting systematic uncertainties are given by the uncertainties in the

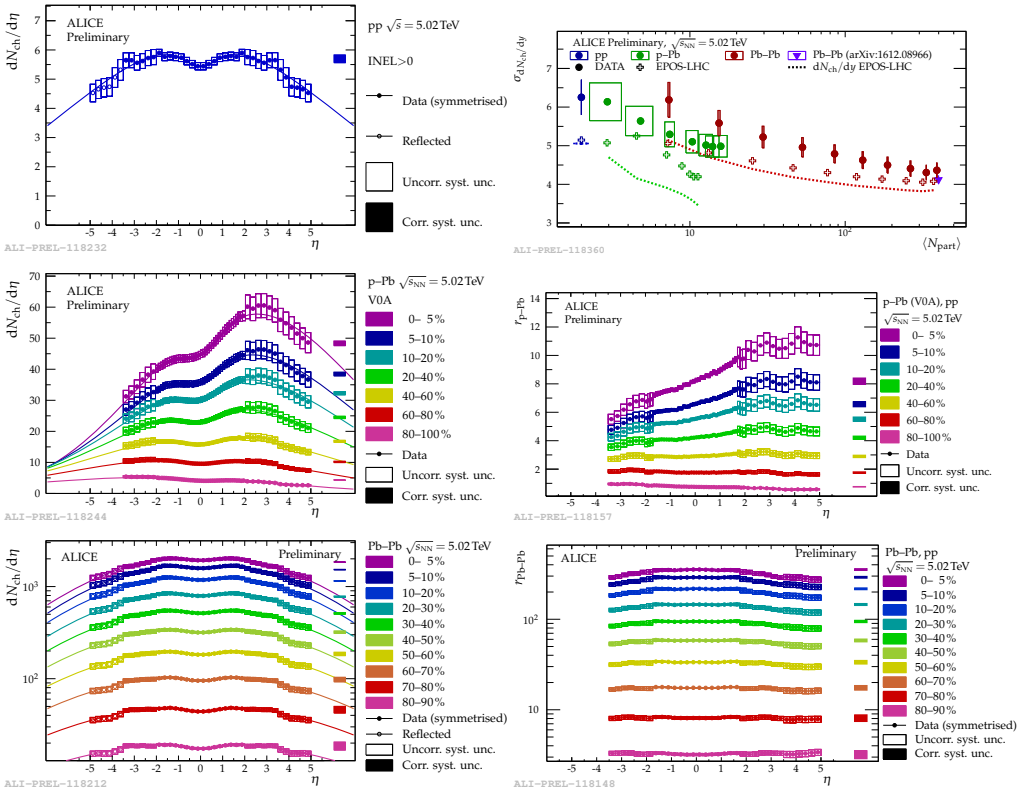

Fig. 1. [Colour online] Left: Charged-particle pseudorapidity density in pp (top), p–Pb (middle), and Pb–Pb (bottom), at a collision energy of $\sqrt{s_{NN}} = 5.02$ TeV. For symmetric collision systems the data has been symmetrized around $\eta = 0$, and the open markers shows the reflection of data into the unmeasured region of $-5 < \eta < -3.5$. Correlated (over η) systematic uncertainties are shown by filled boxes on the right, while uncorrelated systematic uncertainties are shown as open boxes around the points. Statistical errors are insignificant and smaller than the markers. Also shown are best-fit parameterizations of the distributions in terms of Eq. (1) (for pp and Pb–Pb) and Eq. (2) (for p–Pb). Right: The ratio of the charged-particle pseudorapidity density in p–Pb (middle) and Pb–Pb (bottom) to the charged-particle pseudorapidity density in pp collisions at the same collision energy of $\sqrt{s_{NN}} = 5.02$ TeV. Top right: Width of the charged-particle rapidity density distributions for pp, p–Pb, and Pb–Pb collisions at $\sqrt{s_{NN}} = 5.02$ TeV extracted from best-fit parameterizations of the charged-particle pseudorapidity density distributions using Eq. (1) and Eq. (2). Also shown on the figure is a similar evaluation of EPOS-LHC calculations (open markers), and by directly evaluating the width of the EPOS-LHC charged particle rapidity density (dashed lines). Evaluating the width of the charged-particle rapidity density via the full p_T spectra in Pb–Pb at $\sqrt{s_{NN}} = 5.02$ TeV [2] is shown on the far right (down triangle).

$dN_{ch}/d\eta|_X$ measurements. We observe that r_{Pb-Pb} increases for all centrality classes as $|\eta| \to 0$ suggesting narrower distribution with respect to pp, of the particle production in the hot and dense zone produced in heavy–ion collisions. For r_{p-Pb} we see an almost linear rise in the particle production when moving from the p–going to the Pb–going side, indicative of independent proton-nucleon scatterings in the lead-ion side [9, 10]. Similar trends are seen when using less biased centrality estimators, such as ZNA [7].

It has been shown that the charged-particle rapidity density (dN_{ch}/dy), to a very large degree, is Gaussian distributed within the measured region [2, 11]. Those results relied on calculating the average Jacobian $d\eta/dy = \langle J \rangle = \langle \beta \rangle$ using the full p_T spectra of charged pions and kaons, as well as protons and anti-protons. Here, we will take a more simplistic approach by using the approximation $y \approx \eta - \frac{1}{2}\frac{m^2}{p_T^2}\cos\vartheta$, and identify $a = p_T/m$ as the effective ratio of transverse momentum over mass. With this we can write the effective Jacobian as $J'(\eta, a) = 1/\sqrt{1 + \frac{1}{a^2}\frac{1}{\cosh^2\eta}}$. We then make the ansatz that dN_{ch}/dy is Gaussian for symmetric

collision systems (pp and Pb–Pb), so that we can parameterize $\mathrm{d}N_{\mathrm{ch}}/\mathrm{d}\eta$ as

$$f(\eta; A, a, \sigma) = J'(\eta, a)\, A \frac{1}{\sqrt{2\pi}\sigma} e^{-\frac{y^2(\eta,a)}{2\sigma^2}} \quad , \tag{1}$$

where $a = p_{\mathrm{T}}/m$ is the effective transverse momentum over mass ratio, A the total integral of the distribution, σ the width of the distribution, and y the rapidity in the center-of-mass frame. Motivated by the observed almost linear rise in the p–Pb to pp ratios (see right-hand side of Fig. 1), we make the ansatz to replace $A \rightarrow (\alpha y + A)$ for the asymmetric system (p–Pb) and parameterize $\mathrm{d}N_{\mathrm{ch}}/\mathrm{d}\eta$ as

$$g(\eta; A, a, \alpha, \sigma) = J'(\eta, a)\, (\alpha y(\eta, a) + A) \frac{1}{\sqrt{2\pi}\sigma} e^{-\frac{(y(\eta,a)-y_{\mathrm{CM}})^2}{2\sigma^2}} \quad . \tag{2}$$

Best-fit parameterizations of the measured $\mathrm{d}N_{\mathrm{ch}}/\mathrm{d}\eta$ in terms of these two functions are shown in the left-hand side of Fig. 1 for all three collision systems. We observe that the functions Eq. (1) and Eq. (2) describe the measurements quite well within the measured region. That is, the particle production in pp, p–Pb, and Pb–Pb collisions at $\sqrt{s_{\mathrm{NN}}} = 5.02\,\mathrm{TeV}$ is essentially Gaussian in rapidity. The linear modification of the particle production in asymmetric p–Pb collisions is again indicative of independent proton-nucleon scatterings inside the Pb ion [9, 10].

The top-right part of Fig. 1 shows the best-fit values of the Gaussian width ($\sigma_{\mathrm{d}N_{\mathrm{ch}}/\mathrm{d}y}$) for all three collision systems as a function of the number of participating nucleons (N_{part}). The open points and dashed lines on the plot are from evaluations of Eq. (1) and Eq. (2), and direct calculations of $\sigma_{\mathrm{d}N_{\mathrm{ch}}/\mathrm{d}y}$ over EPOS-LHC [12] model calculations. We observe a generally narrower distribution as N_{part} increases, consistent with the ratios $r_{\mathrm{Pb–Pb}}$ to pp. We also see, that the width of the $\mathrm{d}N_{\mathrm{ch}}/\mathrm{d}y$ distributions in p–Pb and Pb–Pb approach that of the pp distribution, which presumably is dominated by kinematic constraints. This suggests an increased particle production near mid-rapidity as an effect of the nuclear medium.

4. Summary

We have measured the charged particle pseudorapidity density in pp, p–Pb, and Pb–Pb collisions at $\sqrt{s_{\mathrm{NN}}} = 5.02\,\mathrm{TeV}$. Direct comparisons as well as parameterisations of the observations in terms of (modified)-Gaussian distributions indicate a collimation of particle production in Pb–Pb collisions, and suggests independent proton-nucleon scatterings within the Pb-ion in p–Pb collisions.

[1] B. Abelev, et al., Performance of the ALICE Experiment at the CERN LHC, Int. J. Mod. Phys. A29 (2014) 1430044.
[2] J. Adam, et al., Centrality dependence of the pseudorapidity density distribution for charged particles in Pb-Pb collisions at $\sqrt{s_{\mathrm{NN}}} = 5.02\,\mathrm{TeV}$, arXiv:1612.08966.
[3] K. Aamodt, et al., Centrality dependence of the charged–particle multiplicity density at mid–rapidity in Pb–Pb collisions at $\sqrt{s_{\mathrm{NN}}} = 2.76\,\mathrm{TeV}$, Phys. Rev. Lett. 106 (2011) 032301.
[4] J. Adam, et al., Charged-particle multiplicities in protonproton collisions at $\sqrt{s} = 0.9$ to 8 TeV, Eur. Phys. J. C77 (1) (2017) 33.
[5] K. Aamodt, et al., Charged–particle multiplicity density at mid–rapidity in central Pb–Pb collisions at $\sqrt{s_{\mathrm{NN}}} = 2.76\,\mathrm{TeV}$, Phys. Rev. Lett. 105 (2010) 252301.
[6] B. Abelev, et al., Centrality determination of Pb-Pb collisions at $\sqrt{s_{\mathrm{NN}}} = 2.76\,\mathrm{TeV}$ with ALICE, Phys. Rev. C88 (2013) 044909.
[7] J. Adam, et al., Centrality dependence of particle production in p-Pb collisions at $\sqrt{s_{\mathrm{NN}}} = 5.02$ TeV, Phys. Rev. C91 (6) (2015) 064905.
[8] J. Adam, et al., Centrality dependence of the charged-particle multiplicity density at midrapidity in Pb-Pb collisions at $\sqrt{s_{\mathrm{NN}}} = 5.02\,\mathrm{TeV}$, Phys. Rev. Lett. 116 (2016) 222302.
[9] S. J. Brodsky, et al., Hadron Production in Nuclear Collisions: A New Parton Model Approach, Phys. Rev. Lett. 39 (1977) 1120.
[10] A. Adil, et al., 3D jet tomography of twisted strongly coupled quark gluon plasmas, Phys. Rev. C72 (2005) 034907.
[11] E. Abbas, et al., Centrality dependence of the pseudorapidity density distribution for charged particles in Pb–Pb collisions at $\sqrt{s_{\mathrm{NN}}} = 2.76\,\mathrm{TeV}$, Phys. Lett. B726 (2013) 610–622.
[12] T. Pierog, et al., EPOS LHC: Test of collective hadronization with data measured at the CERN Large Hadron Collider, Phys. Rev. C92 (2015) 034906.